Preparation of Long TiO_2 Nanotubes from Ultrafine Rutile Nanocrystals

Qinghong Zhang, Lian Gao,* Jing Sun, and Shan Zheng
State Key Laboratory of High Performance Ceramics and Superfine Microstructure, Shanghai Institute of Ceramics, Chinese Academy of Sciences, Shanghai 200050, P. R. China

(Received October 22, 2001; CL-011038)

The morphological dependence of TiO_2 nanotubes on the particle size and crystalline phase of raw materials was observed, and long and uniform TiO_2 nanotubes with lengths up to 500 nm were prepared from rutile TiO_2 nanoparticles (7.2 nm).

Nanostructured TiO_2 materials are of great interest for possible applications to photovoltaic cell,[1] photocatalysts,[2] molecular straws[3] and semiconductor devices where the tuning of the pore size and overall morphology are crucial. Sol-gel method,[4] replica process[5] and template approach[6] have been reported as the procedures for the preparation of oxide nanotubes, and hollow tubes in the diameter of over 100 nm have been created. The orderedly mesoporous TiO_2 materials with pore size of 5 nm were synthesized by modified sol-gel method.[7,8] However, calcination at the temperatures higher than 673 K for decomposition and combustion of templating agents always resulted in the pore collapse and the temperature 673 K was not high enough to improve the crystallinity of the wall of this mesoporous material.[7] Recently, Kasuga et al. treated TiO_2 in the alkaline solution and obtained titanium oxide nanotubes in length of 100 nm.[9] This chemical process opened a novel route to form TiO_2 nanotubes with the crystalline wall. In this work, we used different TiO_2 nanocrystals as raw materials to synthesize TiO_2 nanotubes, and obtained uniform TiO_2 nanotubes in the length up to 500 nm while using 7.2 nm TiO_2 nanocrystals in the rutile phase as the precursor. We found that the morphology of TiO_2 nanotubes was dependent significantly on the particle size and crystalline phase of raw materials.

The preparation of ultrafine TiO_2 in the anatase, rutile and mixed-phases (containing anatase and rutile) has been reported elsewhere.[10] The particle size was altered by calcination at 673 K or 873 K for 2 h and TiO_2 particles in different size and phase were used as raw materials. In a typical process, 100 mg TiO_2 powder was put into a Teflon vessel with 35 mL of 10 M NaOH aqueous solution. The vessel was then placed in a stainless steel vessel, which was closed tightly, and held 383 K for 20 h. The precipitates after hydrothermal treatment were washed well with distilled water and 0.1 M HCl or HNO_3 aqueous solution, then were separated from the washing solution by centrifugation. We found that the nanotubes obtained by washing with dilute HNO_3 were dispersed better in water than those by washing with dilute HCl. Therefore, all nanotubes reported in this paper were obtained by washing with dilute HNO_3 instead of dilute HCl. The washing process was repeated until pH value of the supernatant was lower than 7. Transmission electron microscopy (TEM) images and electron diffraction patterns were obtained on a JEOL–200CX electron microscope. Nitrogen adsorption data were collected on a Micromeritics ASAP 2010 nitrogen adsorption apparatus. The molar Na/Ti ratio was measured by Philips PW2400 X-ray fluorescence spectrometry (XRF).

Table 1. Physicochemical properties of TiO_2 nanocrystals and their derived TiO_2 nanotubes

	Raw materials			Products		
	Phase	S_a[a] /$m^2\ g^{-1}$	d_p[b] /nm	V_p[c] /$cm^3\ g^{-1}$	S_a /$m^2\ g^{-1}$	Decline /$cm^3\ g^{-1}$
R1	R	167.6	7.2	0.782	320.5	57.1
R2	R	32.7	18.5	0.729	181.8	16.3
R3	R	5.0	—	0.537	106.6	7.5
RA	R(58%) A(42%)	77.5	14.2(R) 10.7(A)	0.884	292.9	42.8
A1	A	289.9	4.0	0.878	369.5	30.9
A2	A	183.6	6.8	0.872	451.2	17.1

Notes: R and A denote rutile and anatase, respectively. [a]BET surface area. [b]Represents the particle size in diameter. [c]Pore volume. The decline represents the steep drop from $P/P_0 = 0.50$ to $P/P_0 = 0.45$ in the desorption branch of its N_2 adsorption-desorption isotherms.

The specific surface area, the particle size and the crystalline phase of raw materials, as well as the properties of products after hydrothermal treatment are summarized in Table 1. The molar Na/Ti ratio in nanotubes derived from R1 was 0.13% measured by XRF. The shape of the isotherms of TiO_2 nanotubes, which was inserted in Figure 1, corresponded to the type IV classification with hysteresis, which is a combination of H2 and H1. The H2 type is often associated with a distribution of pore sizes in the mesoporous scale and the area of the hysteresis may be related to the condensation of N_2 in the pore.[11] For the nanotubes prepared from R1, the decline was 57.1 cm^3/g in the region from $P/P_0 =$ 0.50 to 0.45 in the desorption branch of its N_2 adsorption-desorption isotherms, which was much greater than that of mesoporous TiO_2 with high specific surface area and in similar pore size.[7,8] Figure 1 shows the pore size distribution of TiO_2 nanotubes derived from R1, RA, and A2, respectively. The properties of R1, RA, and A2 are described in Table 1. It is notable that most pores have inner diameters of about 4 nm and the pore size distribution of nanotubes prepared from R1 is the narrowest among the three samples, which corresponded to the fact that the length of nanotubes prepared from R1 was the longest. The pore size distribution of nanotubes prepared from RA was narrower than that from A1, but was broader than that from R1. The tubes prepared from A1 were not well defined, corresponding to its wide pore size range from 2 nm to 10 nm.

Figure 2 shows the transmission electron microscopy (TEM) and high-resolution electron microscopy (HREM) images of TiO_2 nanotubes derived from R1. These tubes were in the length up to 500 nm and multiwalled (2–5 layers) with open-ended structure, while no single walled TiO_2 nanotubes were found by HREM observation. The morphology of as-prepared TiO_2 nanotubes was dependent drastically on the particle size and

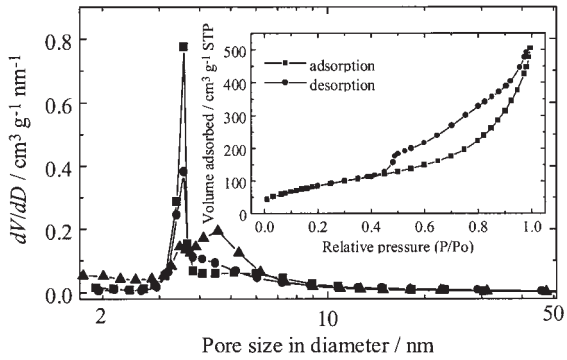

Figure 1. Pore size distribution of TiO_2 nanotubes derived from (■) R1, (●) RA, (▲) A2. The inserted nitrogen isotherms of TiO_2 nanotubes derived from R1 showed a steep decline in its desorption branch in the regoin from $P/P_0 = 0.5$ to 0.45.

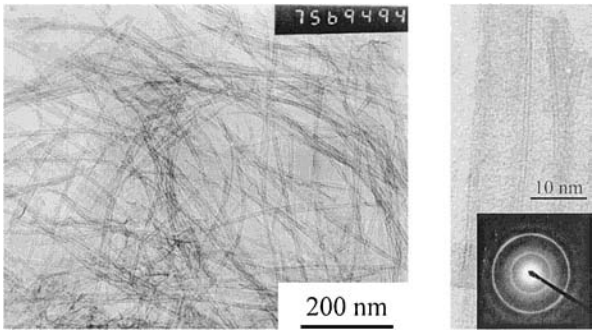

Figure 2. TEM and HREM (right) images of TiO_2 nanotubes derived from R1. the rings of electron diffaction in the inserted electron diffraction patterns was attribute to 101 and 200 diffraction plane of anatase.

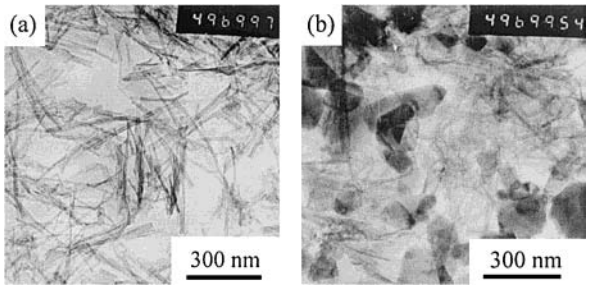

Figure 3. TEM images of TiO_2 nanotubes derived from (a) R2 and (b) R3.

crystalline phase. Figure 3 shows TEM images of nanotubes derived from R2 and R3. The nanotubes derived from R2 were in the length up to 100 nm, which was comparable to that has been reported.[9] While rutile TiO_2 particles (R3) in larger size ($S = 5.0\,m^2/g$) were used as raw materials to synthesize nanotubes, however, some rutile crystals still remained in its product. Both its surface area and the decline in the desorption branch from $P/P_0 = 0.50$ to 0.45 are lower than those of nanotubes derived from R1. These results indicate that the formation of TiO_2 nanotubes is related to particle size of raw materials. Rutile-typed nanocrystals in the ultrafine size have higher surface energy than that in larger size, and higher surface energy may results in crystallites to aggregate. The aggregates in alkaline solution under hydrothermal condition also keep high activity of recrystallizing or self-assembling and to form nanotubes as same as that of well dispersed nanoparticles. The primary particle size of R3 was comparable to the size of aggregates. However, R3 had much lower surface energy and activity, thus, the rate to form nanotubes were low and some particles still remained in the product after hydrothermal treatment. The nanotubes prepared from anatase TiO_2 nanocrystals was poorly defined and it was very difficult to find nanotubes in the products from A1. The nanotubes from A2 were also poorly defined, whose inner pore was not as straight and uniform as that from rutile or mixed-phase TiO_2.[12]

In summary, the crystalline phase, particle size and specific surface area influenced the morphology of the hydrothermal treated TiO_2 nanoparticles significantly. The TiO_2 nanotubes in the length of about 500 nm could be obtained from the ultrafine rutile TiO_2 particles after hydrothermal treatment at 383 K for 20 h. The rutile-to-anatase transformation and recrystallization occurred during the hydrothermal treatment in the concentrated basic medium. The wall of the nanotubes was of multi-layered structure in the anatase phase, and in many cases, the number of layers ranged from 2 to 5. In contrast, the nanotubes formed from ultrafine anatase TiO_2 were poorly defined i.e. the tube was not as straight and uniform as that derived from mixed-phases or rutile TiO_2 particles.

References and Notes

1 U. Bach, D. Lupo, P. Comte, J. E. Moser, F. Welssörtels, J. Scallbeck, H. Spreitzer, and M. Grätzel, *Nature*, **395**, 583 (1998).
2 Q. Zhang, L. Gao, and J. Guo, *Appl. Catal., B*, **26**, 207 (2000).
3 M. R. Pederson and J. Q. Broughton, *Phys. Rev. Lett.*, **69**, 2689 (1992).
4 H. Nakamura and Y. Matsui, *J. Am. Chem. Soc.*, **117**, 2651 (1995).
5 a) P. Hoyer, *Langmuir*, **12**, 1411 (1996). b) H. Imai, Y. Takei, K. Shimizu, M. Matsuda, and H. Hirashima, *J. Mater. Chem.*, **9**, 1971 (1999).
6 a) S. Kobayashi, K. Hanabusa, N. Hamasaki, M. Kimura, and H. Shirai, *Chem. Mater.*, **12**, 1523 (2000). b) C. Hippe, M. Wark, E. Lork, and G. Schulz-Ekloff, *Microporous Mesoporous Mater.*, **31**, 235 (1999). c) D. M. Antonelli, *Microporous Mesoporous Mater.*, **33**, 209 (1999).
7 a) D. M. Antonelli and J. Y. Ying, *Angew. Chem., Int. Ed. Engl.*, **34**, 2014 (1995). b) D. M. Antonelli, *Microporous Mesoporous Mater.*, **30**, 315 (1999). c) Y. Wang, X. Tang, L. Yin, W. Wang, Y. R. Hacohen, and A. Gedanken, *Adv. Mater.*, **12**, 1183 (2000).
8 P. Yang, D. Zhao, D. I. Margolese, B. F. Chmelka, and G. D. Stucky, *Nature*, **396**, 152 (1998).
9 a) T. Kasuga, M. Hiramatsu, A. Hoson, T. Sekino, and K. Niihara, *Langmuir*, **14**, 3160 (1998). b) T. Kasuga, M. Hiramatsu, A. Hoson, T. Sekino, and K. Niihara, *Adv. Mater.*, **11**, 1307 (1999).
10 Q. Zhang, L. Gao, and J. Guo, *Nanostruct. Mater.*, **11**, 1293 (1999).
11 K. S. Sing, D. H. Everett, R. A. Haul, L. Moscou, R. A. Pierotti, J. Rouquerol, and T. Siemieniewska, *Pure Appl. Chem.*, **57**, 603 (1985).
12 The TEM images of nanotubes derived from RA, A1 and A2 were available in the supplementary supporting information.